

# Model for pairing phase transition in atomic nuclei

A. Schiller\*

*Lawrence Livermore National Laboratory, L-414, 7000 East Avenue, Livermore CA-94551*

M. Guttormsen, M. Hjorth-Jensen, J. Rekstad, and S. Siem

*Department of Physics, University of Oslo, N-0316 Oslo, Norway*

A model is developed which allows the investigation and classification of the pairing phase transition in atomic nuclei. The regions of the parameter space are discussed for which a pairing phase transition can be observed. The model parameters include: number of particles, attenuation of pairing correlations with increasing seniority, single particle level spacing, and pairing gap parameter. It is argued that for nuclear models, the pairing phase transition has to be separated in temperature from the signal of the exhaustion of the finite model space.

PACS number(s): 05.20.Gg, 05.70.Fh, 21.10.Ma, 24.10.Pa

## I. INTRODUCTION

Phase transitions in small systems are an important research topic. One of the most interesting problems in this context is probably the question of the existence and classification of a possible phase transition from a hadronic phase to a quark-gluon plasma in high energy physics. The answer to this question has far-reaching consequences into many other fields of research like, e.g., cosmology, since it has been argued that hadronization of the quark-gluon plasma should be a first-order phase transition in order to allow for possible supercooling and consequently the emergence of large scale inhomogeneities in the cosmos within the inflationary big-bang model [1].

In nuclear physics, two different phase transitions have been discussed in the literature. A first-order phase transition has been reported in the multifragmentation of nuclei [2], thought to be the analogous phenomenon in a finite system to a liquid-gas phase transition in the thermodynamical limit. A pivotal role in these studies is played by the presence of a convex intruder in the microcanonical entropy curve [3,4]. This leads to a negative branch of the microcanonical heat capacity which is used as an indicator of a first-order phase transitions in small systems. Negative heat capacities have indeed been observed in the multifragmentation of atomic nuclei, though the heat capacity curve has not been derived directly from the caloric curve, but by means of energy fluctuations [2,5]. Another finding of a negative branch of the heat capacity curve has been in sodium clusters of 147 atoms [6], indicating a possible first-order phase transition. On the other hand, it is not clear whether the observed negative heat capacities are simply due to the changing volume of the system under study that is progressively evaporating particles [7]. It has also been

suggested that a negative heat capacity can be observed when studying a system in a metastable state [8]. In general, great care should be taken in the proper extraction of temperatures and other thermodynamical quantities of a multifragmenting system [9,10].

A further difficulty in characterizing the order of a phase transition in a finite system using negative heat capacities arises from the fact that there are no counterparts in the thermodynamical limit. For this reason, no simple connection with the Ehrenfest classification of phase transitions can be made. Therefore, it is not clear that a phenomenon involving negative heat capacities in small systems is analogous to a first-order phase transition in the thermodynamical limit. Another way to classify phase transitions for finite systems has been proposed within the canonical ensemble. This classification scheme is based on the distribution of zeros (DOZ) of the canonical partition function in the complex temperature plane [11] and has successfully been applied to a model of multifragmentation [12]. This classification scheme reduces to the Ehrenfest classification in the thermodynamical limit and is applicable for first, second, and higher order phase transitions.

The second phase transition discussed for atomic nuclei has been anticipated for the transition from a phase with strong pairing correlations to a phase with weak pairing correlations [13]. Early schematic calculations have shown that pairing correlations can be quenched by temperature as well as by the Coriolis force in rapidly rotating nuclei [14–17]. This makes the quenching of pairing correlations in atomic nuclei very similar to the breakdown of superfluidity in  $^3\text{He}$  (due to rapid rotation and/or temperature) or of superconductivity (due to external magnetic fields and/or temperature). Recently, structures in the heat capacity curve related to the quenching of pairing correlations have been obtained

---

\*Electronic address: Andreas.Schiller@llnl.gov

within the relativistic mean field theory [18,19], the finite-temperature random phase approximation (RPA) [20], the finite-temperature Hartree-Fock-Bogoliubov theory [21], and the shell-model Monte Carlo (SMMC) approach [22–26]. An S-shaped structure in the heat capacity curve could also be observed experimentally [27] and has been interpreted as a fingerprint of a second-order phase transition from a phase with strong pairing correlations to a phase with weak pairing correlations. Indeed, the analogy of the quenching of pairing correlations in atomic nuclei with the breakdown of superfluidity in  $^3\text{He}$  and the breakdown of superconductivity suggests a second order phase transition and a schematic calculation might support this assumption [28]. Interestingly, similar structures of the heat capacity curve as observed for atomic nuclei in [27] have been seen in small metallic grains undergoing a second-order phase transition from a superconductive to a normal conductive phase [29], thereby supporting the analogous findings for atomic nuclei. On the other hand, breaking of nucleon pairs has been experimentally shown to cause a series of convex intruders in the microcanonical entropy curve of deformed rare earth nuclei [30,31], leading to several negative branches of the microcanonical heat capacity. This finding might, in analogy to the discussion of nuclear multifragmentation, be taken as an indicator of several first-order phase transitions. Interpreting the quenching of pairing correlations as a series of first-order phase transitions seems, however, physically unattractive and might rather suggest that a negative branch of the microcanonical heat capacity curve does not necessarily indicate the analogous phenomenon in a small system to a first-order phase transition in the thermodynamical limit. A similar conclusion has been drawn by the authors of Ref. [28].

We will in this work develop a model for the atomic nucleus which allows us to investigate the occurrence and classification of the pairing phase transition in atomic nuclei as a function of particle number and other parameters within the model. In order to do so, we will apply the classification scheme of Borrmann *et al.* [11,12] to the pairing phase transition.

## II. STATISTICAL ENSEMBLES

The proposed nuclear model is formulated within the canonical ensemble theory although the microcanonical ensemble theory might, at a first glance, be the more appropriate ensemble for describing the nucleus below the particle threshold. At low excitation energies, the nucleus can be regarded as a closed system with respect to energy and particle exchange. However, the microcanonical ensemble theory, just because it requires a closed system, has an inherent conceptual problem when it comes to small systems of few particles. Within the microcanonical ensemble theory one has

$$T(E) = \left( \frac{\partial S(E)}{\partial E} \right)_V^{-1}. \quad (1)$$

For macroscopic systems, it can be proven experimentally that  $T$  from this equation equals the thermodynamical temperature defined by primary and secondary temperature standards, like the triple point of water. Unfortunately, for small systems, this experimental proof can in principle not be performed due to the following difficulty. Temperature measurements involve necessarily energy exchange between the system and the thermometer in order to bring the thermometer to the same temperature as the system under study, thus undermining the requirement of a closed system for a microcanonical description. For macroscopic systems, this problem is solved by introducing a small thermometer compared to the system. For small systems of a few particles, in general, every thermometer will, due to its size, act as a heat bath when brought into contact with the system under study. Thus, temperature measurements on small, truly microcanonical systems seem virtually impossible and, therefore, it cannot be proven that the quantity  $T$  from Eq. (1) corresponds to the thermodynamical temperature in these cases, although  $S$  and  $E$  are still well defined and can be measured. It should also be noted that all means of temperature measurements which are based on the application of the statistical theory, like momentum distribution measurements, are not valid either, since the connection between the microcanonical statistical theory and thermodynamics is always based on Eq. (1).

The treatment of the nucleus in the canonical ensemble theory has also the advantage that a classification scheme for phase transitions exists which reduces to the Ehrenfest definition in the thermodynamical limit [11,12]. Hence, the difficulties mentioned in the Introduction can be overcome. Although it was suggested in [3,4] that the canonical ensemble theory should not be applied to first-order phase transitions, it has been shown that it gives convincing results in the case of nuclear multifragmentation [12] which is thought to be a first-order phase transition. It has also been objected that the Laplace transformation involved in the canonical ensemble theory smears out the thermodynamical information of the system under study and that the canonical partition function therefore contains less information than the microcanonical partition function [3]. We want to emphasize, however, that the partition function of the canonical ensemble, when known on all of the right-hand half of the complex temperature plane, certainly does carry as much thermodynamical information of the system as the microcanonical partition function. The reason for this is that the inverse Laplace transformation (from the canonical to the microcanonical partition function) is mathematically defined in a unique fashion and hence the microcanonical partition function can in principle be recovered unanimously. However, since the inverse Laplace transformation requires integration on the complex tem-

perature plane along a parallel to the imaginary axis, one has to expect that knowledge of the canonical partition function over all of the right hand half of the complex temperature plane is pivotal for revealing the complete thermodynamical information of the system under study. The classification scheme [11,12] which we intend to apply in this work, is based on the DOZ of the canonical partition function and therefore complies with this requirement.

### III. MODEL

The model in this work is a further development of the previously proposed model in [32,33]. We will first recapitulate those features of the old model which we have adopted in the present work and then describe the changes and additions. The basic idea behind our model is the assumption of a reservoir of nucleon pairs. These nucleon pairs can be broken and the unpaired nucleons are then promoted into an infinite, equidistant, doubly degenerated single-particle level scheme. The nucleon pairs in the reservoir do not interact with each other and are thought to occupy an infinitely degenerated ground state. The nucleons in the single particle level scheme do not interact with each other either, but they have to obey the Pauli principle. The model is depicted in Fig. 1. The essential parameters of the model are: the number of pairs in the reservoir at zero temperature  $N$ , the spacing of the single-particle level scheme  $\epsilon$ , and the energy necessary to break a nucleon pair  $2\Delta$ . Quenching of pairing correlations is introduced into this model by reducing the required energy to break a nucleon pair in the presence of unpaired nucleons. We assume that for every already broken nucleon pair, the energy to break a further nucleon pair is reduced by a factor  $r \leq 1$ . Thus, in the presence of  $p$  broken nucleon pairs, the energy to break the  $(p+1)$ th nucleon pair is reduced to  $2r^p\Delta$ . We assume further that the single unpaired nucleon in an odd nucleus reduces the necessary energy for breaking the first nucleon pair of the same species to  $2\sqrt{r}\Delta$ .

The proposed model is supposed to display three distinct phases: a phase where pairing correlations dominate, a phase where the pairs have essentially been broken up and the system behaves like a non-interacting Fermi-gas dominated by Pauli-blocking, and a phase where the nucleons become diluted in a phase space much larger in size (in terms of the number of realizations of thermal excitations) than the number of nucleons present. In this third phase, the Pauli blocking can be neglected and the system resembles mostly a classical ideal gas. We will, in the following, denote the three phases

as the paired phase, the unpaired phase, and the quasi-classical phase. The three distinct phases of the system makes it possible to investigate two different phase transitions with our model.

It has been shown previously [32], that the partition function for  $n$  unpaired nucleons in an infinite, equidistant, doubly degenerated single-particle level scheme can be written as

$$z_n = \sum_{i=0}^{(n-1)/2} 2 z_{n-i}^\uparrow z_i^\uparrow \quad n = \text{odd} \quad (2)$$

$$z_n = \sum_{i=0}^{(n-2)/2} 2 z_{n-i}^\uparrow z_i^\uparrow + (z_{n/2}^\uparrow)^2 \quad n = \text{even}, \quad (3)$$

where the  $z_i^\uparrow$  are the partition functions for  $i$  spin-up nucleons in an infinite, equidistant, non-degenerated single-particle level scheme. The  $z_i^\uparrow$  can be expressed by means of the recursive formula [32]

$$z_0^\uparrow = 1 \quad (4)$$

$$z_{i+1}^\uparrow = z_i^\uparrow \frac{\exp(-i\epsilon\beta)}{1 - \exp(-(i+1)\epsilon\beta)}, \quad (5)$$

where  $\beta = 1/T^1$ . According to our model, in order to promote  $n$  nucleons from the reservoir into the single-particle level scheme, one has to break  $p = n/2$  nucleon pairs which requires the energy

$$2\Delta + 2r\Delta + 2r^2\Delta + \dots + 2r^{p-1}\Delta = 2\Delta \frac{1-r^p}{1-r} \quad (6)$$

in the even case. In the odd case, one has to multiply this energy by  $\sqrt{r}$  in order to take into account the quenching effect of the odd nucleon. Hence, the partition function for  $n$  unpaired nucleons in our model becomes

$$Z_n = z_n \exp(-2\sqrt{r}\Delta \frac{1-r^{(n-1)/2}}{1-r} \beta) \quad n = \text{odd} \quad (7)$$

$$Z_n = z_n \exp(-2\Delta \frac{1-r^{n/2}}{1-r} \beta) \quad n = \text{even}. \quad (8)$$

In order to obtain the partition function for the complete system, one has to sum over all possible numbers of unpaired nucleons in the single-particle level scheme. Thus, the partition function of our model is finally

$$Z_{\text{pair}} = \sum_{n=1}^{N+1} Z_{2n-1} \quad \text{odd} \quad (9)$$

$$Z_{\text{pair}} = \sum_{n=0}^N Z_{2n} \quad \text{even}. \quad (10)$$

---

<sup>1</sup>Here, and in the following, we set Boltzmann's constant  $k_B = 1$ .

At this point, the average number of unpaired particles can be calculated in a straightforward manner

$$\langle n \rangle = \sum_{n=1}^{N+1} n Z_{2n-1} / \sum_{n=1}^{N+1} Z_{2n-1} \quad \text{odd} \quad (11)$$

$$\langle n \rangle = \sum_{n=0}^N n Z_{2n} / \sum_{n=0}^N Z_{2n} \quad \text{even.} \quad (12)$$

The number of unpaired particles will fluctuate, and the fluctuations can be calculated by

$$\delta n = \sqrt{\langle n^2 \rangle - \langle n \rangle^2}, \quad (13)$$

where  $\langle n^2 \rangle$  is given by

$$\langle n^2 \rangle = \sum_{n=1}^{N+1} n^2 Z_{2n-1} / \sum_{n=1}^{N+1} Z_{2n-1} \quad \text{odd} \quad (14)$$

$$\langle n^2 \rangle = \sum_{n=0}^N n^2 Z_{2n} / \sum_{n=0}^N Z_{2n} \quad \text{even.} \quad (15)$$

Since there are protons and neutrons in the nucleus, one has to create two partition functions  $Z_{\text{pair}}$ , one for every nucleon species, and multiply them with each other. Here, one can introduce different parameters  $\epsilon$ ,  $\Delta$ ,  $r$ , and  $N$  for protons and neutrons. For the sake of simplicity, we will, however, in this work not make use of this possibility<sup>2</sup>. In addition to the model partition function, we have in the previous work [33] also assumed a rotational and vibrational partition function

$$Z_{\text{rot}} = \sum_{I=0,2,4,\dots}^{12} \exp(-A_{\text{rig}} I(I+1)\beta) \quad (16)$$

$$Z_{\text{vib}} = \sum_{\nu=0}^1 3^\nu \exp(-\nu \hbar \omega_{\text{vib}} \beta) \quad (17)$$

with  $A_{\text{rig}}$  being the rigid-body rotational parameter and  $\omega_{\text{vib}}$  the vibrational frequency of the nucleus under study. The nuclear partition function becomes therefore in the most general case

$$Z = Z_{\text{pair}}^\pi Z_{\text{pair}}^\nu Z_{\text{rot}} Z_{\text{vib}} \quad (18)$$

where we will use in this work equal proton and neutron partition functions  $Z_{\text{pair}}^\pi$  and  $Z_{\text{pair}}^\nu$ . We would like to stress that for  $r = 1$ , the present model is approximately equal to the previous model [32,33], whereas the possibility of  $r < 1$ , i.e., the quenching of pairing correlations, is a new feature of the present model.

---

<sup>2</sup>This means that the even-odd and the odd-even systems will be equal. We will, therefore, in this work use the term 'odd system' to denote either of the two.

Although the model is purely phenomenological, we would like to emphasize that it can be closely related to a microscopical model. If one assumes a Hamiltonian of the form

$$\hat{H} = \hat{H}_\pi + \hat{H}_\nu + \hat{H}_{\text{rot}} + \hat{H}_{\text{vib}} \quad (19)$$

with

$$\hat{H}_{\pi,\nu} = \epsilon \sum_{\kappa} a_{\kappa}^{\dagger} a_{\kappa} - |G| \sum_{\kappa,\lambda>0} a_{\kappa}^{\dagger} a_{-\kappa}^{\dagger} a_{-\lambda} a_{\lambda}, \quad (20)$$

i.e., a simple single-particle plus pairing Hamiltonian for protons and neutrons, and conventional rotational and vibrational Hamiltonians  $\hat{H}_{\text{rot}}$  and  $\hat{H}_{\text{vib}}$  for the collective modes, similar results as in this work can be achieved [28,34]. The advantage of the present, phenomenological model over the microscopic model is that, in general, a much larger number of particles and single-particle levels can be taken into account.

#### IV. MODEL PROPERTIES

It has already been shown that the previous model [32,33] describes well the level density and heat capacity in the <sup>162</sup>Dy nucleus. Further, it could reproduce [33] the anchor points of the level density curve proposed in [32] for several other mid-shell nuclei. However, in order to do so, one had to assume values for  $\epsilon$  which were off general estimates of the shell model. Also, it was not possible to reproduce the theoretical heat capacity curve of iron nuclei as calculated in [26] within the SMMC approach. Since in the new model an additional parameter is introduced, we have the hope to use more reasonable values of  $\epsilon$  and still be able to describe the experimental data with good accuracy.

The parameters for the present nuclear model are taken from the following systematics [35]

$$\epsilon = \frac{3\pi^2}{A} \text{ MeV}, \quad (21)$$

where the level density parameter  $a = \pi^2/3\epsilon$  is related to the mass number  $A$  by  $a = A/9 \text{ MeV}^{-1}$ . The pairing-gap parameter  $\Delta$  can also be related to the mass number  $A$  by

$$\Delta = \frac{12}{\sqrt{A}} \text{ MeV}. \quad (22)$$

The rigid-body rotational parameter  $A_{\text{rig}}$  can be expressed in terms of the rigid moment of inertia  $\Theta_{\text{rig}}$  by

$$A_{\text{rig}} = \hbar^2/2 \Theta_{\text{rig}}. \quad (23)$$

Assuming the nucleus to be a rotational symmetric ellipsoid of constant density, the rigid moment of inertia can be expressed by the nuclear mass  $M$  and mean radius  $R$  as  $\Theta_{\text{rig}} = 2/5 MR^2$ . The nuclear mean radius can then again be related to the mass number by  $R = 1.24 \text{ fm } A^{1/3}$ . The vibrational frequency of the nucleus can be taken directly from spectroscopic data [36]. For the parameter  $r$  of our model, which governs the evolution of the pairing gap  $\Delta$  with temperature, no systematics exist. Theoretical studies suggest a quenching of the pairing energy per broken pair in the order of 0.56 in the mass 190 region [37] yielding a  $\Delta(T)$  curve comparable to results from modern RPA calculations [38] (see Fig. 2). Probably  $r$  will increase with mass number. This effect is, however, not taken into account in this work and we adopt  $r = 0.56$  for all nuclei studied. Finally, for the last parameter  $N$  of the model, we assume ten neutron and ten proton pairs in the reservoir at zero temperature in most of this work. This is an increase over the previous calculations [32,33] where a total number of ten nucleon pairs was assumed. The increase of the number of nucleon pairs in the reservoir allows us to map thermodynamical quantities of nuclei up to higher temperatures of, e.g., 1.5 MeV in dysprosium. A summary of the applied parameters is listed in Table I.

In order to compare the model to experimental data, one has to calculate experimentally observed quantities like the free energy  $F$ , the entropy  $S$ , the caloric curve  $\langle E(T) \rangle$ , the heat capacity  $C_V$ , and the nuclear level density  $\rho(\langle E \rangle)$  from the canonical partition function. While the first four quantities can be calculated in a straightforward fashion by the following expressions

$$F = -T \ln Z \quad (24)$$

$$S = - \left( \frac{\partial F}{\partial T} \right)_V \quad (25)$$

$$\langle E \rangle = F + ST \quad (26)$$

$$C_V = \left( \frac{\partial \langle E \rangle}{\partial T} \right)_V, \quad (27)$$

the nuclear level density should, in principle, be obtained by an inverse Laplace transformation of the canonical partition function. We will, however, in this work make use of the saddle-point approximation [23]

$$\rho(\langle E \rangle) = \frac{\exp(S)}{T \sqrt{2\pi C_V}}, \quad (28)$$

which gives satisfactory results for the nuclear level density [33]. Finally, we will calculate the average number of unpaired nucleons  $\langle n \rangle$ , the fluctuation of this number  $\delta n$ , and the effective, temperature-dependent pairing energy  $\Delta(T) = r^{(n/2)} \Delta(0)$ .

In Fig. 2, thermodynamical quantities derived from the model are shown using parameters for  $^{162}\text{Dy}$ . The quantities  $S$ ,  $\langle n \rangle$ ,  $C_V$  and  $\Delta(T)$  are coinciding for the even-even, odd, and odd-odd systems above temperatures of 0.8–1 MeV, indicating that the pairing correlations are already completely quenched at these temperatures. Indeed, the heat capacity curve displays a linear dependence on temperature between  $T = 1$  and 1.5 MeV, which is the expected temperature dependence for a Fermi gas. The fluctuation of the number of unpaired particles  $\delta n$  increases strongly around  $T \sim 0.5$  MeV, which coincides with a strong decrease of the effective pairing energy  $\Delta(T)$  and the S-shape of the heat capacity curve, first observed experimentally in [27]. The latter three observations can be interpreted as signatures of a second-order phase-transition like phenomenon in nuclei.

On the right-hand panels of Fig. 2, the quantities  $\langle n \rangle$  and  $C_V$  can be seen to split up again for the even-even, odd, and odd-odd systems at temperatures above 1.5–2 MeV. At these temperatures, all nucleons start to become excited, the reservoir is rapidly being exhausted and the system can no longer absorb energy at the same rate without getting heated up rapidly. Therefore, the heat capacity decreases until it reaches the limit of  $1 k_B$  per particle<sup>3</sup> and the number of unpaired particles will increase at a progressively smaller pace to the limit of 40, 41, and 42 for the even-even, odd, and odd-odd systems, respectively. This is the signal of a possible second phase transition inherent in the model from an unpaired phase to a quasi-classical phase. It is not expected that this second phase transition is present in the experimental data since the nuclei under study in this work have more particles than are included in the model space. Therefore, the second phase transition in the model merely reflects the fact that the model space is still too small in order to describe heavy nuclei adequately at the highest temperatures<sup>4</sup>. Some kind of signal of the exhaustion of the model space will, however, be present in all types of

<sup>3</sup>This corresponds to the value for a two-dimensional ideal, classical gas.

<sup>4</sup>In any case, atomic nuclei become unbound, undergo multi-fragmentation and therefore lose their identities at the critical temperature for the liquid-gas phase transition. This will therefore be the temperature beyond which our model becomes unrealistic, even when including all nucleons of the nucleus.

nuclear model calculations which do not include all nucleons or the complete single-particle level scheme. We will therefore investigate in Sect. VB whether and how the truncation of the model space interferes with the signal of the pairing phase transition.

Figure 3 shows how the model compares to the level-density anchor points of Ref. [32] and the measured level densities of two dysprosium isotopes [27]. The data points for the dysprosium isotopes have been modified slightly for the purpose of this work. While in the previous works [27,39] a back-shifted level-density formula with the von Egidy parameterization [40] was used for normalization and extrapolation to the neutron-binding energy and beyond, in this work, we will make use of a simple, shifted level-density formula

$$\rho = f \frac{\exp(2\sqrt{aU})}{12\sqrt{0.1776} a^{1/2} U^{3/2} A^{1/3}} \quad (29)$$

with  $U = E - \Delta$ ,  $a = A/9 \text{ MeV}^{-1}$  and  $\Delta = 12/\sqrt{A} \text{ MeV}$  for consistency. The parameterization for the spin cut-off parameter  $\sigma$  is taken from Ref. [41] and the normalization parameter  $f$  is chosen such that the level-density formula intersects the data point from neutron resonance spacing [42]. It is satisfying that the model reproduces the data points well without any fine tuning of the parameters in the different mass regions off closed shells. Only in the case of the iron mass region, the single particle level spacing had to be increased from the systematic value of  $\epsilon = 517 \text{ keV}$  to  $800 \text{ keV}$  in order to describe the data. The shortcomings of the model to reproduce the iron data using parameters from the systematics is most likely due to the presence of the double shell closure in the neighboring  $^{56}\text{Ni}$  isotope. Irregularities of both, the single-particle level spacing (or more precisely the closely related level-density parameter  $a$ ) and the pairing-gap parameter  $\Delta$  in the vicinity of closed shells are a well-known fact [35]. We would like to stress that a better fit to the experimental data might certainly be achieved by fine tuning of the parameters for protons and neutrons for every mass region. However, the possibility of using systematic parameters for the model highlights its general applicability.

In Fig. 4, the model predictions are compared to published canonical thermodynamical quantities. For the iron nuclei these data are recent SMMC calculations [26], while for the dysprosium nuclei, semi-experimental data exist [27]. The comparison is made for canonical heat-capacity curves, since these curves are effectively second derivatives of the canonical partition functions and therefore more sensitive to structural changes in the nucleus than any other thermodynamical quantities.

Although the steepness of the S-shape differs somewhat and the absolute value at the plateau is off by  $\sim 30\%$ , the overall agreement of the model calculation for the dysprosium nuclei with the semi-experimental data is satisfying. Especially the temperature where the steepness of the S-curve reaches the maximum, i.e., the critical temperature of the pairing phase transition, is well reproduced. For

the iron nuclei, the agreement between our model and the SMMC calculations is not so good. Unfortunately, no experimental data exists to compare the two models to, therefore it is difficult to judge which is the more realistic one. While the present model is very schematic, it offers the possibility to include infinitely many single-particle levels and much more nucleons than the SMMC calculations. Especially the necessity of a finite single-particle level scheme in SMMC calculations will cause the heat capacity curve to approach zero for high temperatures and it is not clear at which temperature this effect takes over in the data of Ref. [26]. On the other hand, the SMMC calculation can incorporate shell-effects in a more natural way than by simply adjusting the two parameters  $\epsilon$  and  $\Delta$ . Especially the use of a realistic nucleon-nucleon interaction and the correct single particle energies for the complete ( $pf + 0g_{9/2}$ ) shell might change the picture significantly at low temperatures compared to the present schematic model.

In conclusion, it can be stated that the present model, using a systematic parameter set, reproduces fairly well the available experimental data, but a discrepancy with SMMC calculations in the iron-mass region exists. Since the agreement with experiment is good in the rare earth mass region, where also experimental data is abundant, we are confident that the model can be applied to classify the order of the pairing phase transition with good accuracy in deformed rare earth nuclei if not in most mid-shell nuclei.

## V. CLASSIFICATION OF PHASE TRANSITIONS

### A. Classification scheme

The classification scheme for phase transitions is based entirely on [11,12] and is only slightly modified for the purpose of this work. We will therefore only recapitulate briefly the main features of the classification scheme. The scheme relies on the DOZ and derives three quantities, where two of them classify the order of a possible phase transition and the third one reflects the discreteness of the system under study.

First, we define the inverse complex temperature

$$\mathcal{B} = \beta + i\tau, \quad (30)$$

where  $\beta = 1/T$  as usual and  $\tau$  denotes the imaginary part of the inverse complex temperature which is measured in  $\text{MeV}^{-1}$  in this work. The zeros of the canonical partition function typically line up on curves through the complex temperature plane. Whenever such a curve intersects the real axis, a phase transition in the system might occur. Figure 5 shows a typical example with four zeros on a curve approaching the real axis. The zeros are denoted by  $(\beta_j, \tau_j)$  with  $j = 1 \dots 4$  and  $j$  increasing with increasing distance from the real axis.

The angle  $\nu$ , being the first quantity of interest, is calculated by

$$\nu = \arctan \frac{\beta_2 - \beta_1}{\tau_2 - \tau_1}. \quad (31)$$

Further, the average inverse distance between zeros can be calculated as

$$\Phi = \frac{1}{2} \left( \frac{1}{d_{j-1}} + \frac{1}{d_j} \right), \quad (32)$$

where  $d_j = \sqrt{(\beta_{j+1} - \beta_j)^2 + (\tau_{j+1} - \tau_j)^2}$ . The function  $\Phi$  can then be approximated in the vicinity of the real axis by a power law of  $\tau_j$  only

$$\Phi(\tau_j) \propto \tau_j^\alpha, \quad (33)$$

such that the second quantity of interest,  $\alpha$ , can be calculated by means of

$$\alpha = \frac{\ln \Phi(\tau_3) - \ln \Phi(\tau_2)}{\ln \tau_3 - \ln \tau_2}. \quad (34)$$

One can easily see that in order to calculate  $\alpha$ , one has to determine at least the first four zeros closest to the real axis. With a slight redefinition of the function  $\Phi$  by

$$\tilde{\Phi}(\tilde{\tau}_j) = \frac{1}{d_j}, \quad (35)$$

where  $\tilde{\tau}_j = (\tau_j + \tau_{j+1})/2$ , only the first three zeros have to be known. The order of the phase transition is now completely determined by the two quantities  $\nu$  and  $\alpha$ . When  $\alpha < 0$  or  $\alpha = \nu = 0$  the system exhibits a first-order phase transition. For  $0 < \alpha < 1$  and  $\nu = 0$  or  $\nu \neq 0$ , a second-order phase transition takes place. For  $\alpha > 1$  the phase transition is of higher order.

The third parameter  $\tau_1$  indicates the discreteness of the system. More precisely, the quantity  $\tau_1/\hbar$  equals the time after which an ensemble of equal systems loses its memory. Only if  $\tau_1 \rightarrow 0$  for increasing particle numbers, one has a corresponding phase transition in the Ehrenfest sense for the thermodynamical limit. For finite systems, one can then speak of a phase transition in the generalized Ehrenfest sense. Finally,  $\beta_1$  might be defined as the inverse of the critical temperature of the phase transition. In the following, the classification scheme will be applied to the DOZ of mid-shell nuclei calculated within the proposed nuclear model.

## B. Results

First, we investigate the effect of the numbers of pairs in the reservoir at zero temperature on the DOZ. On the upper left panel in Fig. 6, the calculation is done for one single pair in the reservoir. Certainly, no phase transition can be claimed, but the positions of the zeros already indicate at which temperatures the pairing phase transition

will take place. Also, the effect of the Pauli blocking by the single unpaired nucleon is visible, shifting the zero of the odd system to higher temperatures. For two pairs in the reservoir, two zeros for the even and odd system can be seen. The zeros are positioned on slanted lines where the zeros of the odd system are again shifted to higher temperatures due to the Pauli blocking. The same is true for three pairs in the reservoir. According to the previous subsection, three zeros in a line can already be used to classify a phase transition. In the present case, since  $\alpha$  is negative, a first-order phase transition is indicated. Due to the small size of the system, however, one cannot attribute this phase transition simply to the quenching of pairing correlations. Rather, one has to acknowledge the fact that the pairing phase transition coincides with the phase transition from an unpaired to a quasi-classical system, giving rise to a disturbed signal for the order of the phase transition. This becomes clearer in the case of four pairs in the reservoir. Here, one might already discuss two separate phase transitions, since one can distinguish two different curves of zeros approaching the real axis. While the curves to the right might be attributed to the pairing phase transition, the curves to the left are indicating the transition to a quasi-classical phase. Still, since the two curves are sharing zeros one cannot expect to get a clean signal for the classification of the two phase transitions and indeed for both curves one obtains negative values of  $\alpha$ , indicating two first order phase transitions, a result which is at variance with expectations. First the calculation with seven pairs separates the two phase transitions enough in temperature to get clean signals. Here, one finds negative values of  $\alpha$  for the transitions to a quasi-classical phase, indicating a first-order phase transition. Interestingly, this phase transition does show only a very small odd-even effect, which can in total be attributed to the by one higher particle number in the odd case. The pairing phase transition, however, has a large odd-even dependence and yields  $\alpha \sim 0.86$  for the even case, indicating a second-order phase transition and a value greater than one for the odd case, indicating a higher order phase transition. This result remains stable for larger particle numbers. The values of  $\nu$  are consistent with the conclusions drawn above.

We will now investigate the evolution of the parameters  $\beta_1$ , i.e., the inverse critical temperatures of the respective phase transitions, as function of  $N$ , i.e., the size of the model space. In the upper left panel of Fig. 7, it is shown that  $\beta_1$  for the phase transition from the unpaired to the quasi-classical phase obeys a power law of the form  $aN^b$  with  $b \sim -1$ . This means that in the thermodynamical limit the critical temperature of this phase transition will approach infinity and thus, the phase transition cannot be observed in infinitely large systems. This is not surprising, since the very nature of this phase transition, which is a transition from a Fermi gas to a quasi-classical phase where the nucleons are diluted in phase space, obviously requires increasingly higher temperatures the more nucleons are present. Here, we want to stress once more

that this phase transition is a true phase transition inherent in the model and might even be realized in nature by some physical system. However, when applying the model to heavy nuclei which are much larger than the model space,  $\beta_1$  merely indicates at which (inverse) temperature the reservoir is being exhausted and that the model space is too small to describe heavy nuclei adequately below  $\beta_1$ . Eventually, the temperature beyond which our model becomes unrealistic, even when including all nucleons of the nucleus in the model space, is given by the critical temperature for the liquid-gas phase transition (see also <sup>4</sup>).

On the lower left panel of Fig. 7, the evolution of  $\beta_1$  for the pairing phase transition as function of the size of the model space is shown. The inverse critical temperature  $\beta_1$  of the pairing phase transition is independent of the size of the model space as it is expected, but it shows a pronounced odd-even effect due to the Pauli blocking of the single unpaired nucleon.

Finally, we will investigate the parameters  $\tau_1$  as function of  $N$  in order to gain information on whether the phase transitions observed in the finite system under study correspond to true phase transitions in the thermodynamical limit. Unfortunately, in the case of the first-order phase transition from the unpaired phase to the quasi-classical phase,  $\beta_1$  and therefore also  $\tau_1$  show a trivial scaling with  $N$  which is clouding the relevant, additional  $N$  dependence of  $\tau_1$ . Therefore, one has to investigate the dimensionless parameter  $\tau_1/\beta_1$  for a residual, non-trivial  $N$  dependence in order to be able to conclude on the reality of the phase transition in the generalized Ehrenfest sense for the finite system. On the upper right panel of Fig. 7 the dependence of  $\tau_1/\beta_1$  on  $N$  for the phase transition from the unpaired to the quasi-classical phase is shown to obey the power law  $aN^b$  with  $b \sim -0.5$ . Thus, the dimensionless parameter  $\tau_1/\beta_1$  is shown to approach the real axis in the thermodynamical limit and the modeled phase transition satisfies the generalized Ehrenfest definition of a phase transition.

For the pairing phase transition, one could in principle investigate  $\tau_1$  directly as function of  $N$ , since  $\beta_1$  is independent of  $N$  and thus, no trivial scaling of  $\tau_1$  with  $N$  will alter the results. However, to treat everything on an equal footing, also in this case, we have investigated the dimensionless parameter  $\tau_1/\beta_1$ . Since  $\tau_1/\beta_1$  shows no sign of approaching the real axis (see the lower right panel of Fig. 7), one has to ask the question whether the modeled pairing phase transition corresponds to any true phase transition in the thermodynamical limit.

In order to answer this question, we introduce the notion that, in the case of the pairing phase transition, the size of the system is not determined by the size of the reservoir  $N$ , but rather by the mass number  $A$  and subsequently by the mass-number-dependent parameters  $\epsilon$  and  $\Delta$ . Specifically, the parameter  $g = \Delta/\epsilon$  scales as  $\sqrt{A}$  and should thus be increased in order to model a larger system. This is in sharp contrast to the analysis in [28], where the authors assume that the simple increase of the

number of particles  $N$  in the calculation should model heavier nuclei.

Therefore, in order to investigate the evolution of  $\tau_1$  for the pairing phase transition with respect to the relevant size of the system, i.e., the mass number  $A$ , we have calculated the DOZ for nuclei in four different mass regions (see Fig. 8). Obviously, the pairing phase transition can only be observed for nuclei with mass numbers  $A > 100$  within the presented model, since for lighter nuclei, the curve of zeros relevant for the quenching of pairing correlations points away from the real axis, and therefore, one cannot claim, within the model, the existence of a pairing phase transition for light nuclei. On the left-hand panel of Fig. 9, the inverse critical temperature of the pairing phase transition is shown to scale approximately with  $A^{2/3}$  in the rare-earth mass region, which is expected when assuming  $T_c = \Delta/S_1$ , where  $S_1$  is the single-particle entropy [32]. The iron data do not quite follow this trend, since we have used a single-particle level spacing for the iron nuclei outside the global systematics of Eq. (21), see also Table I. Again, by investigating the dimensionless parameter  $\tau_1/\beta_1$  of the pairing phase transition, the trivial mass dependence is taken out and the residual dependence of  $\tau_1/\beta_1$  on  $A$  will tell if the modeled pairing phase transition in the finite system under study is a phase transition in the generalized Ehrenfest sense. On the right-hand panel of Fig. 9, this residual  $A$  dependence of  $\tau_1/\beta_1$  has been fitted by the power law  $aA^b$  with  $b \sim -1/3$ , again omitting the iron data due to their unsystematic value of  $\epsilon$ . Thus,  $\tau_1/\beta_1$  will approach the real axis for large mass numbers. Therefore, one can conclude that the modeled pairing phase transition is a true phase transition in the generalized Ehrenfest sense, provided that one investigates this phase transition with respect to the relevant size of the system, which is the mass number  $A$  rather than the size of the model space  $N$ . As a final remark, it is interesting to notice that the odd-even difference of  $\beta_1$  and  $\tau_1/\beta_1$  becomes smaller with increasing mass number. Thus, in the thermodynamical limit, it will not matter if the system consists of an even or an odd number of particles, as it is expected.

## VI. CONCLUSIONS

We have developed a model which allows the investigation of phase transitions in a small system of two or more particles. The anticipated phase transition from a paired to an unpaired system in rare earth nuclei could be produced. The order of the modeled pairing phase transition could be determined for even systems to be of second order and for odd systems to be of higher order. A second phase transition, which is of first order, is inherent in the model and connects the unpaired and a quasi-classical phase. The latter phase is characterized by the dilution of particles in phase space and might therefore be encountered in systems where the phase space is much larger in



size (in terms of the number of realizations of thermal excitations) than the number of particles present. This second phase transition is a true phase transition and might be realized in nature by some physical system. In the case of modeling heavy nuclei with particle numbers much larger than the model space, however, it reflects merely the fact that the model space is still too small in order to describe those nuclei adequately at high temperatures (within the limits discussed in <sup>4</sup>). It has been shown that the pairing phase transition and the signal of the exhaustion of the finite model space have to be carefully separated in temperature in order to obtain a clear signature of the pairing phase transition in atomic nuclei. The presented model is able to take into account a sufficient number of single-particle levels and nucleons to allow a good separation and to display conclusive evidence of the pairing phase transition in heavy mid-shell nuclei.

### ACKNOWLEDGMENTS

Part of this work was performed under the auspices of the U.S. Department of Energy by the University of California, Lawrence Livermore National Laboratory under Contract No. W-7405-ENG-48. Financial support from the Norwegian Research Council (NFR) is gratefully acknowledged. We thank David Dean and Paul Garrett for interesting discussions and Emel Tavukcu for carrying out some preliminary calculations for this work.

- 
- [1] Pawel Danielewicz, private communication.
- [2] M. D’Agostino *et al.*, Phys. Lett. B **473**, 219 (2000).
- [3] D. H. E. Gross, Phys. Rep. **279**, 119 (1997).
- [4] D. H. E. Gross and E. V. Votyakov, Eur. Phys. J. B **15**, 115 (2000).
- [5] Ph. Chomaz, V. Duflot, and F. Gulminelli, Phys. Rev. Lett. **85**, 3587 (2000).
- [6] Martin Schmidt, Robert Kusche, Thomas Hippler, Jörn Donges, Werner Kronmüller, Bernd von Issendorff, and Hellmut Haberland, Phys. Rev. Lett. **86**, 1191 (2001).
- [7] L. G. Moretto, J. B. Elliott, L. Phair, and G. J. Wozniak, preprint nucl-th/0012037.
- [8] C. Tsallis, B.J.C. Cabral, A. Rapisarda, and V. Latora, preprint cond-mat/0112266.
- [9] J. Pochodzalla, *et al.*, in Proceedings of the 1st Catania Relativistic Ion Studies: Critical Phenomena and Collective Observables, Acicastello, Italy, 1996, page 1 (World Scientific, Singapore).
- [10] S. Das Gupta, A. Z. Mekjian, and M. B. Tsang, Michigan State University preprint MSUCL-1178 (2000).
- [11] Peter Borrmann, Oliver Mülken, and Jens Harting, Phys. Rev. Lett. **84**, 3511 (2000).
- [12] Oliver Mülken and Peter Borrmann, Phys. Rev. C **63**, 024306 (2001).
- [13] Mitsuo Sano and Shuichiro Yamasaki, Progr. Theor. Phys. **29**, 397 (1963).
- [14] Alan L. Goodman, Nucl. Phys. **A352**, 30 (1981).
- [15] Alan L. Goodman, Nucl. Phys. **A352**, 45 (1981).
- [16] K. Tanabe and K. Sugawara-Tanabe, Phys. Lett. B **97**, 337 (1980).
- [17] K. Tanabe and K. Sugawara-Tanabe, Nucl. Phys. **A390**, 385 (1982).
- [18] B. K. Agrawal, Tapas Sil, J. N. De, and S. K. Samaddar, Phys. Rev. C **62**, 044307 (2000).
- [19] B. K. Agrawal, Tapas Sil, S. K. Samaddar, and J. N. De, Phys. Rev. C **63**, 024002 (2001).
- [20] Nguyen Dinh Dang, Z. Phys. A **335**, 253 (1990).
- [21] J. L. Egido, L. M. Robledo, and V. Martin, Phys. Rev. Lett. **85**, 26 (2000).
- [22] D. J. Dean, S. E. Koonin, K. Langanke, P. B. Radha, and Y. Alhassid, Phys. Rev. Lett. **74**, 2909 (1995).
- [23] H. Nakada and Y. Alhassid, Phys. Rev. Lett. **79**, 2939 (1997).
- [24] S. Rombouts, K. Heyde, and N. Jachowicz, Phys. Rev. C **58**, 3295 (1998).
- [25] J. A. White, S. E. Koonin, and D. J. Dean, Phys. Rev. C **61**, 034303 (2000).
- [26] S. Liu and Y. Alhassid, Phys. Rev. Lett. **87**, 022501 (2001).
- [27] A. Schiller, A. Bjerve, M. Guttormsen, M. Hjorth-Jensen, F. Ingebretsen, E. Melby, S. Messelt, J. Rekstad, S. Siem, and S. W. Ødegård, Phys. Rev. C **63**, 021306(R) (2001).
- [28] A. Belić, D. J. Dean, and M. Hjorth-Jensen, preprint cond-mat/0104138.
- [29] Bent Lauritzen, Andrea Anselmino, P. F. Bortignon and Ricardo A. Broglia, Ann. Phys. (NY) **223**, 216 (1993).
- [30] E. Melby, L. Bergholt, M. Guttormsen, M. Hjorth-Jensen, F. Ingebretsen, S. Messelt, J. Rekstad, A. Schiller, S. Siem, and S. W. Ødegård, Phys. Rev. Lett. **83**, 3150 (1999).
- [31] E. Melby, M. Guttormsen, J. Rekstad, A. Schiller, S. Siem, and A. Voinov, Phys. Rev. C **63**, 044309 (2001).
- [32] M. Guttormsen, M. Hjorth-Jensen, E. Melby, J. Rekstad, A. Schiller, and S. Siem, Phys. Rev. C **63**, 044301 (2001).
- [33] M. Guttormsen, M. Hjorth-Jensen, E. Melby, J. Rekstad, A. Schiller, and S. Siem, Phys. Rev. C **64**, 034319 (2001).
- [34] M. Guttormsen, A. Bjerve, M. Hjorth-Jensen, E. Melby, J. Rekstad, A. Schiller, S. Siem, and A. Belić, Phys. Rev. C **62**, 024306 (2000).
- [35] A. Bohr and B. Mottelson, *Nuclear Structure* (Benjamin, New York, 1969), Vol. I.
- [36] R. Firestone and V.S. Shirley, *Table of Isotopes*, 8th ed. (Wiley, New York, 1996).
- [37] T. Døssing, *et al.*, Phys. Rev. Lett. **75**, 1276 (1995).
- [38] N. Dinh Dang and V. Zelevinsky, Phys. Rev. C **64**, 064319 (2001).
- [39] A. Schiller, L. Bergholt, M. Guttormsen, E. Melby, J. Rekstad, and S. Siem, Nucl. Instrum. Methods Phys. Res. A **447**, 498 (2000).
- [40] T. von Egidy, H. H. Schmidt, and A. N. Bekhami, Nucl. Phys. **A481**, 189 (1987).
- [41] A. Gilbert and A. G. W. Cameron, Can. J. Phys. **43**,

1446 (1965).

[42] *Handbook for Calculations of Nuclear Reaction Data*

(IAEA, Vienna, IAEA-TECDOC-1024, 1998).

TABLE I. The model parameters have been calculated by means of  $\epsilon = 30 \text{ MeV}/A$ ,  $\Delta = 12 \text{ MeV}/\sqrt{A}$ , and  $A_{\text{rig}} = 34 \text{ MeV } A^{-5/3}$  with the exception of  $\epsilon$  for  $^{58}\text{Fe}$  (see text). All values are rounded to integer numbers. The values for  $\hbar\omega_{\text{vib}}$  have been taken from spectroscopic data of Ref. [36]. The value of  $r = 0.56$  is suggested for the mass 190 region by the calculations of Ref. [37] and adopted for all four nuclei in this work.

Nucleus	$\epsilon$ [keV]	$\Delta$ [keV]	$A_{\text{rig}}$ [keV]	$\hbar\omega_{\text{vib}}$ [MeV]	$r$
$^{58}\text{Fe}$	800	1576	39	2.0	0.56
$^{106}\text{Pd}$	283	1166	14	1.4	0.56
$^{162}\text{Dy}$	185	943	7	0.9	0.56
$^{234}\text{U}$	128	784	4	0.8	0.56

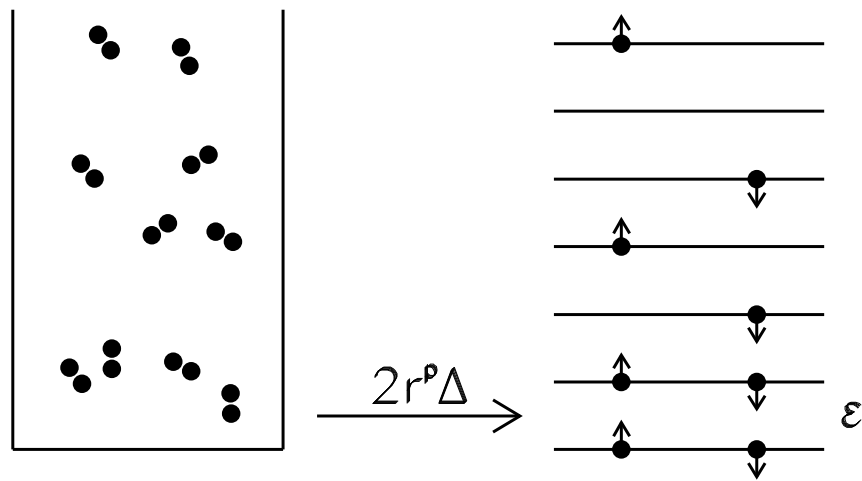


FIG. 1. Schematic representation of the nuclear model. For details, see text.

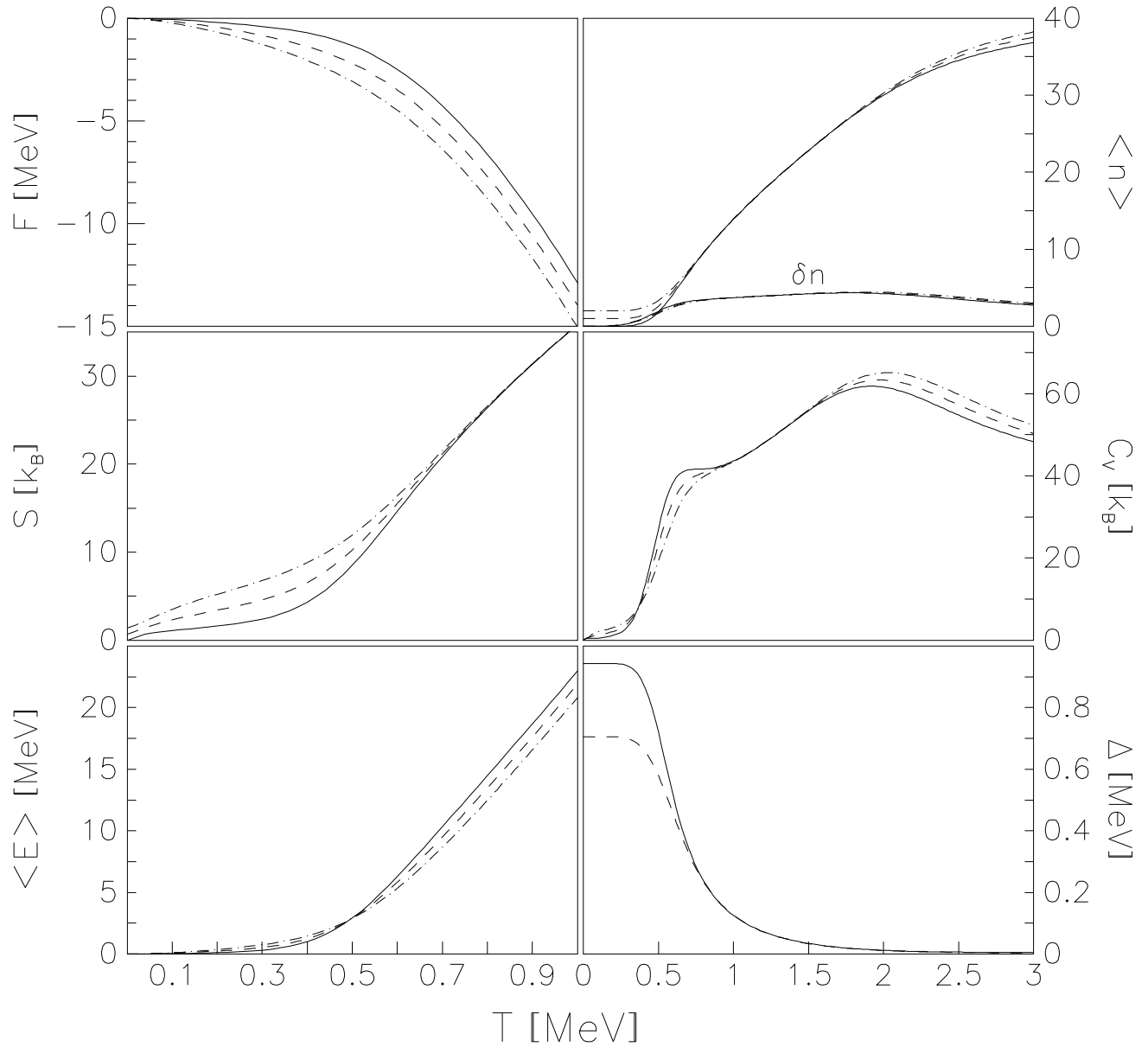


FIG. 2. Thermodynamical quantities calculated within the nuclear model. The solid, dashed, and dash-dotted lines are for the even-even, odd, and odd-odd system, respectively. For  $\Delta(T)$ , only the even and odd case for one nucleon species is shown. The long tail of the  $\Delta(T)$  curves at high temperatures agrees well with modern RPA calculations [38]. The parameters are those for  $^{162}\text{Dy}$ .

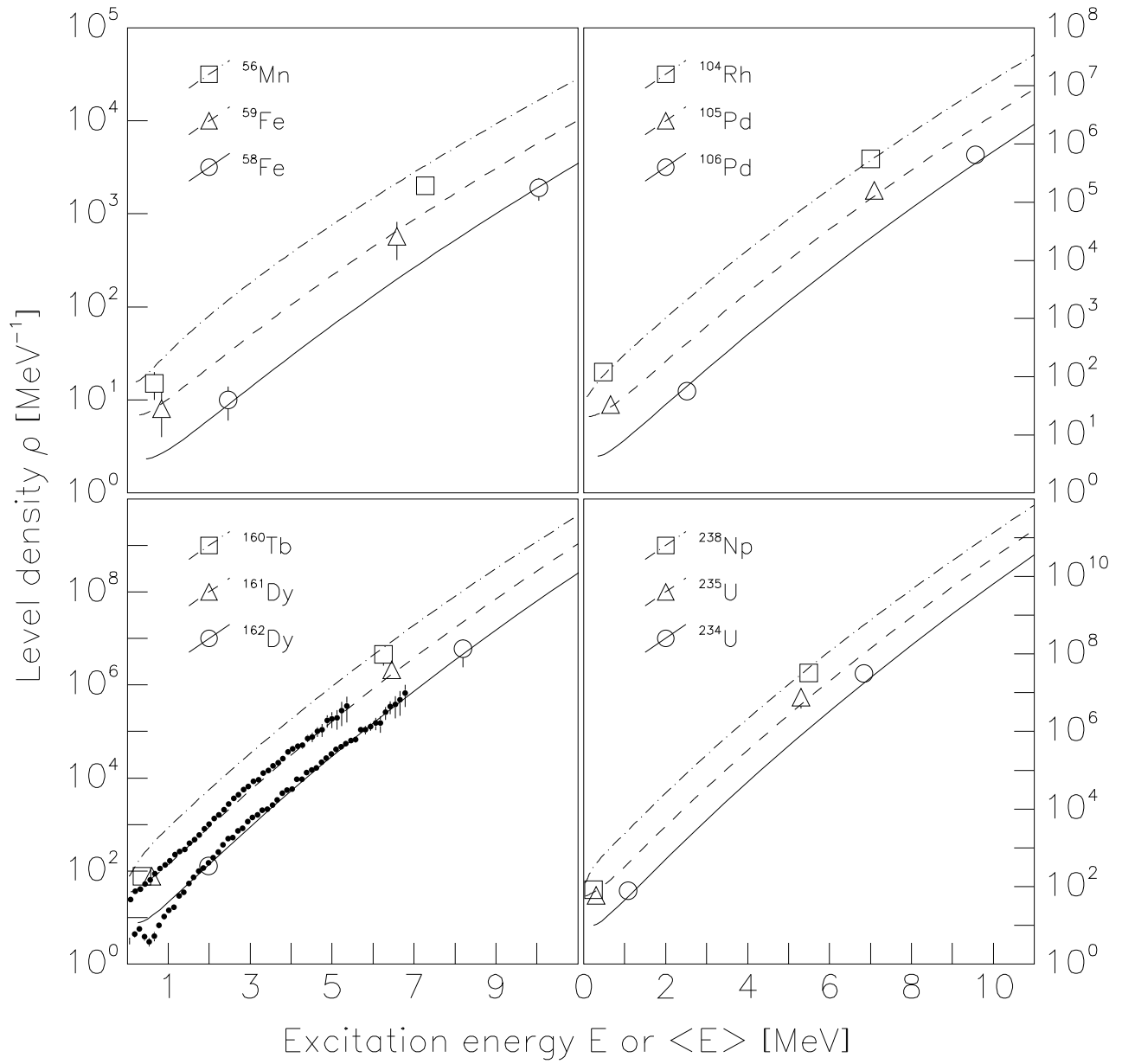


FIG. 3. Comparison of calculated and experimental level density. The open symbols are the anchor points of Ref. [32], the full symbols are the experimental level densities of Ref. [27] using a slightly different normalization (see text).

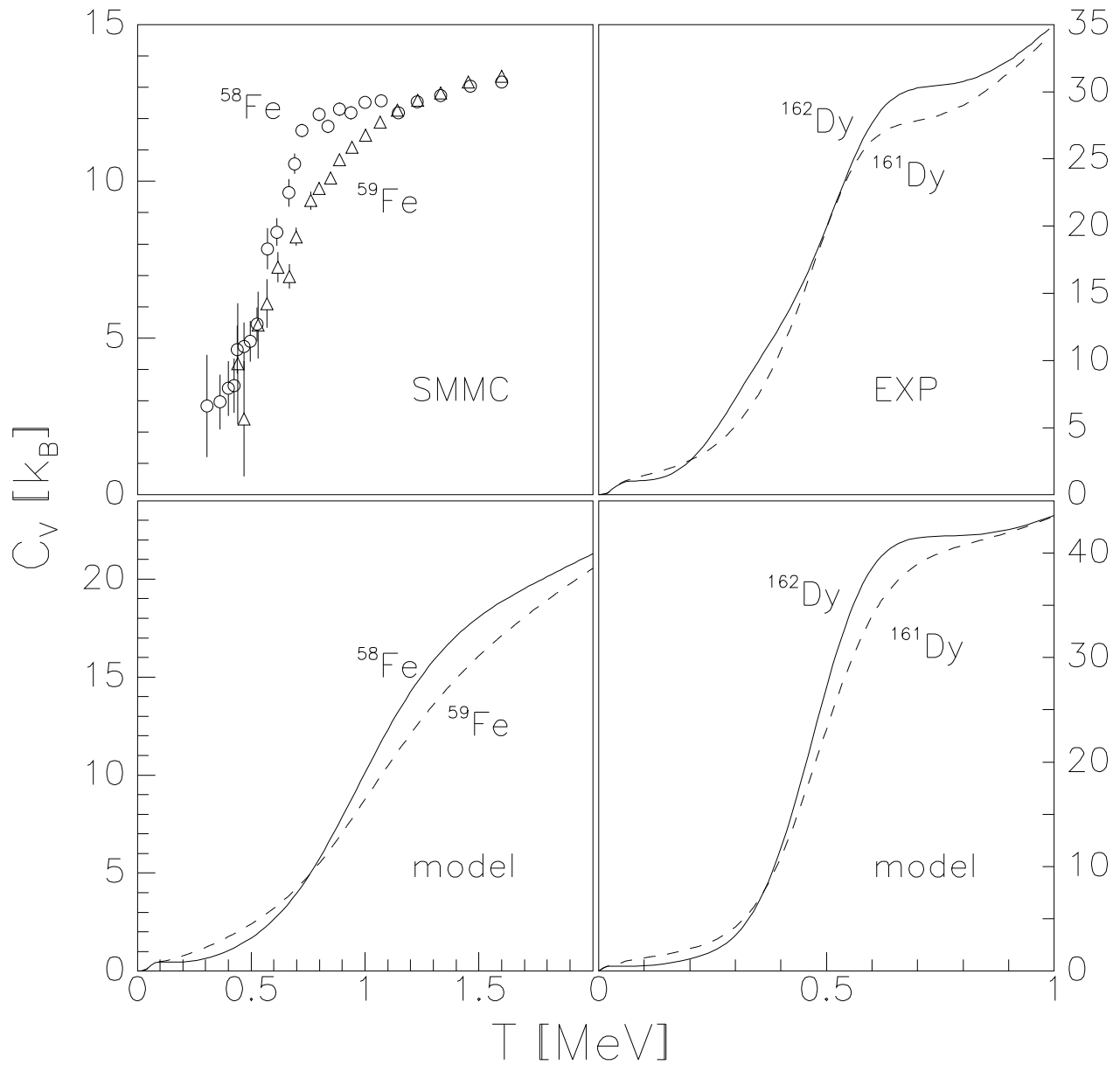


FIG. 4. Comparison of heat capacity curves of the present model and of other publications. The open symbols are scanned from Ref. [26], the data for the dysprosium nuclei are from Ref. [27] using a slightly different normalization (see text).

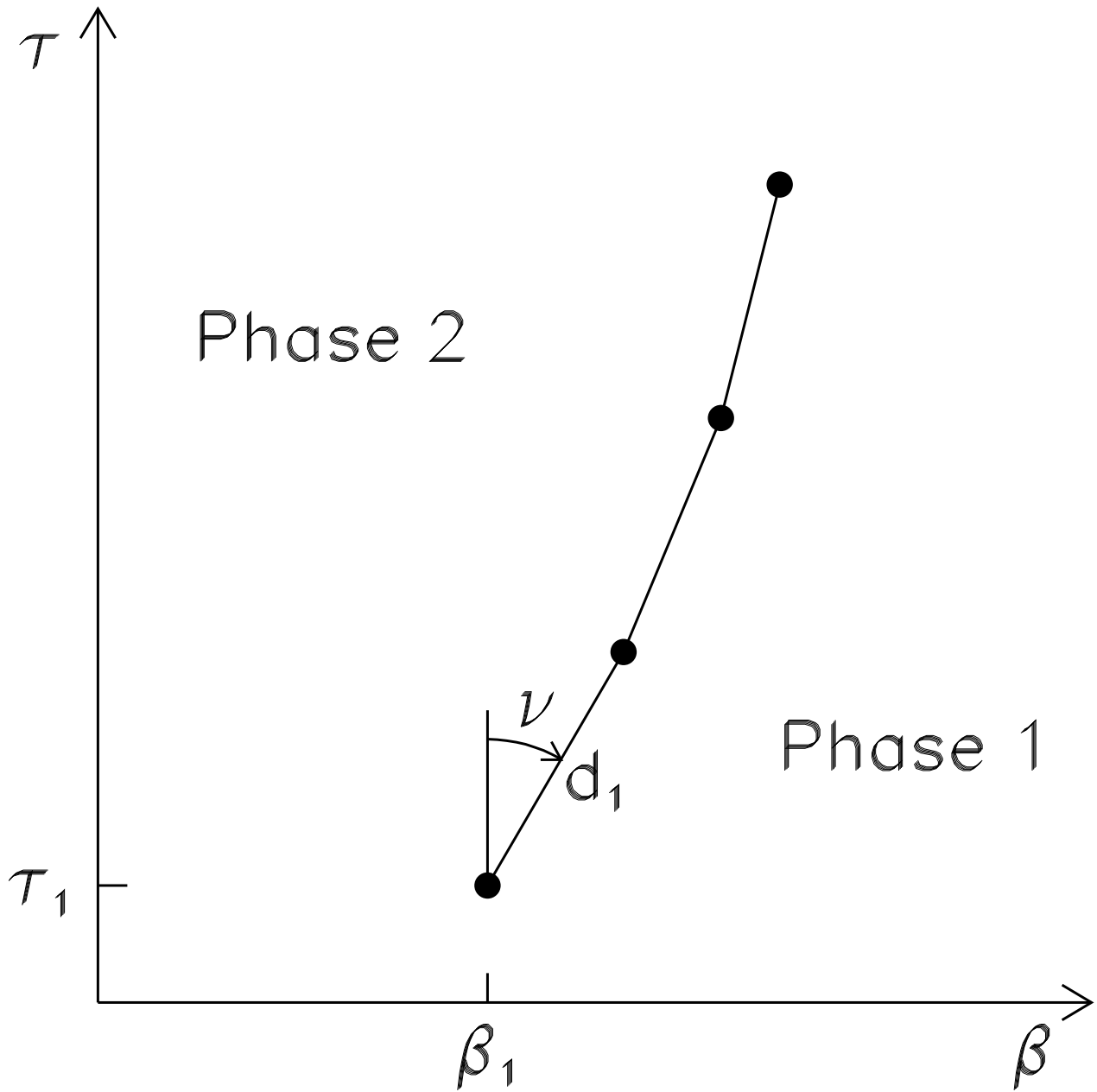


FIG. 5. Definition of important quantities for the classification of phase transitions in finite systems.



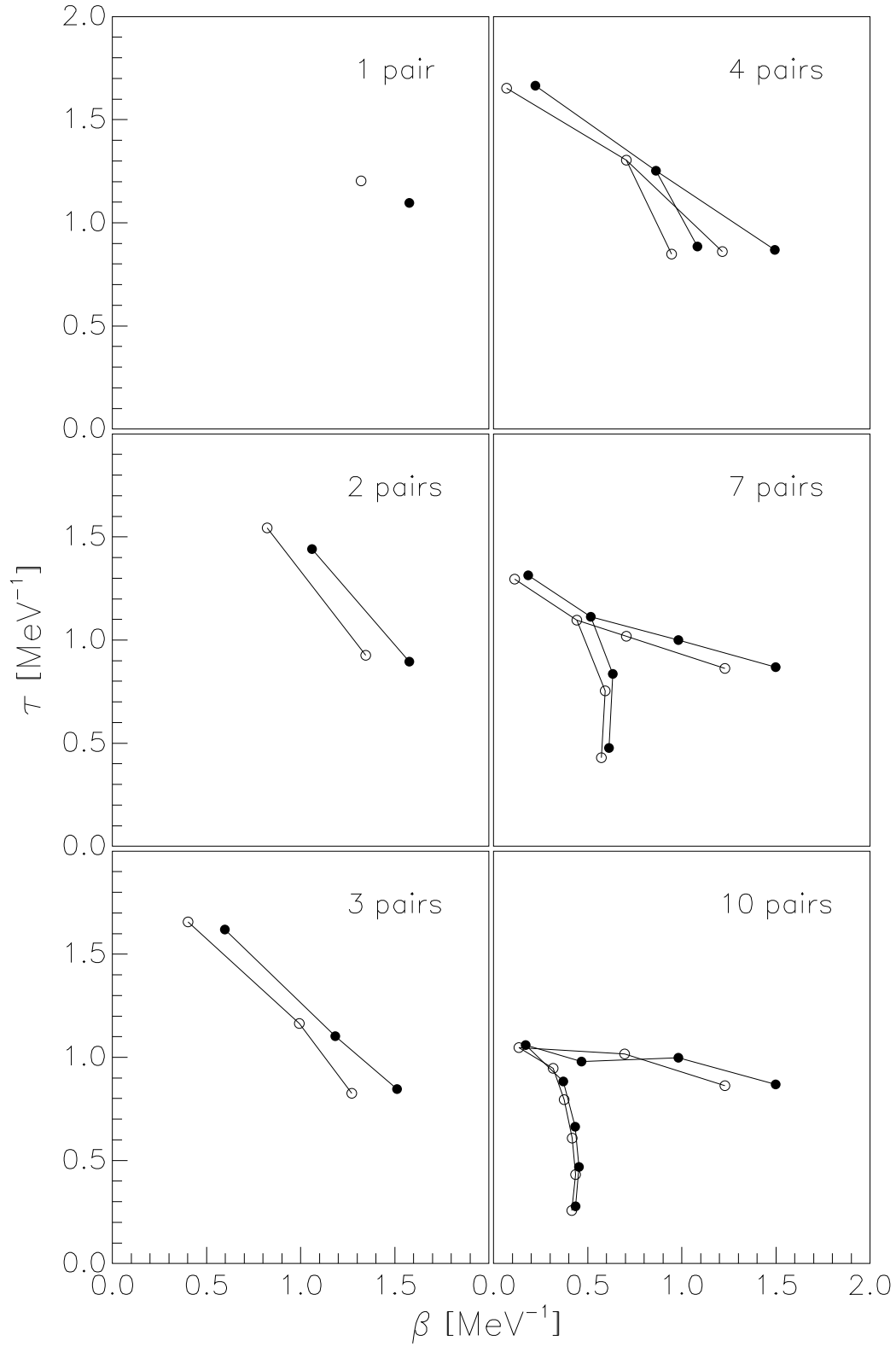


FIG. 6. DOZ for different numbers of pairs in the reservoir. The full symbols are for the even system, the open symbols for the odd system. The parameters of the model are those for <sup>162</sup>Dy. There exist zeros with  $\tau > 2$  MeV<sup>-1</sup> and/or  $\beta < 0$  MeV<sup>-1</sup>, but these are not of interest in this context.

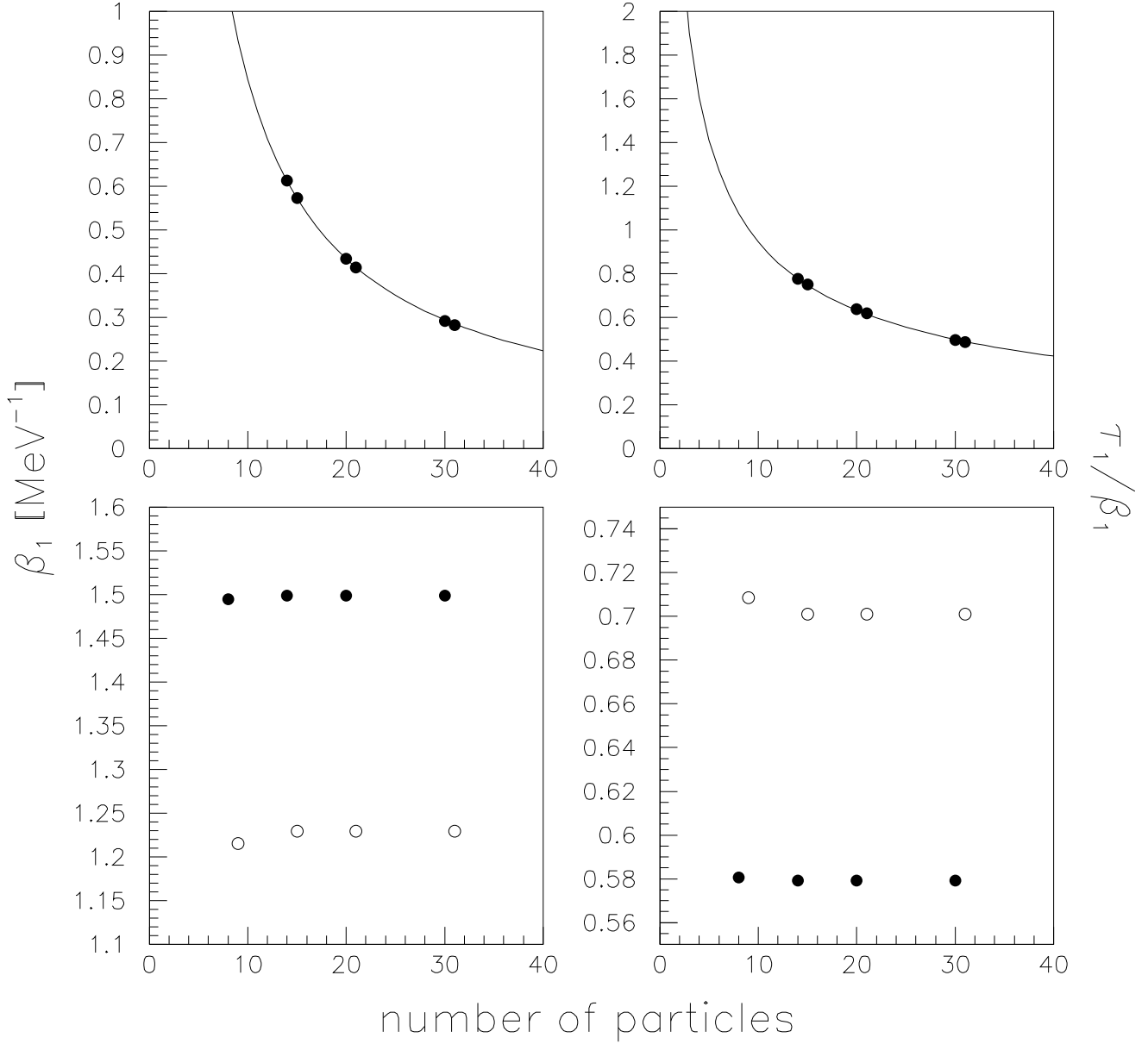


FIG. 7. Evolution of the parameters  $\beta_1$  and  $\tau_1/\beta_1$  as function of the size of the model space for the two phase transitions. Upper panels: the phase transition from the unpaired to the quasi-classical phase. Lower panels: the pairing phase transition. The full symbols in the lower panels are for the even system, the open symbols are for the odd system. The curves on the upper panels are fits to the data by a simple power law. The odd and even systems align on identical curves.

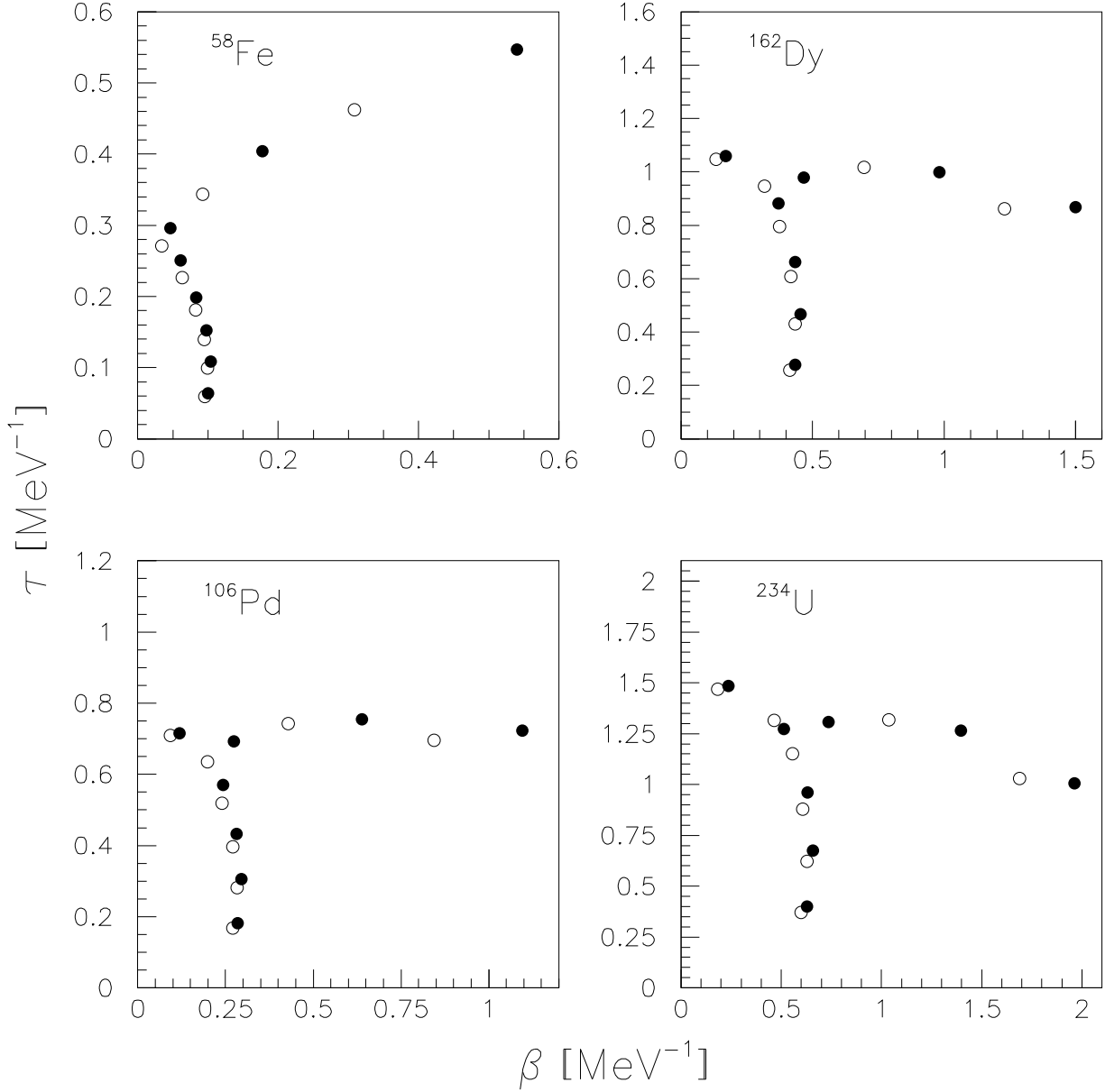


FIG. 8. DOZ for nuclei in four different mass regions. The full symbols are for the even systems, the open symbols stand for the odd systems. The line of zeros approaching the real axis perpendicularly corresponds to the exhaustion of the finite model space and is not relevant in the discussion. Only the more or less horizontal lines of zeros reflect the quenching of pairing correlations.

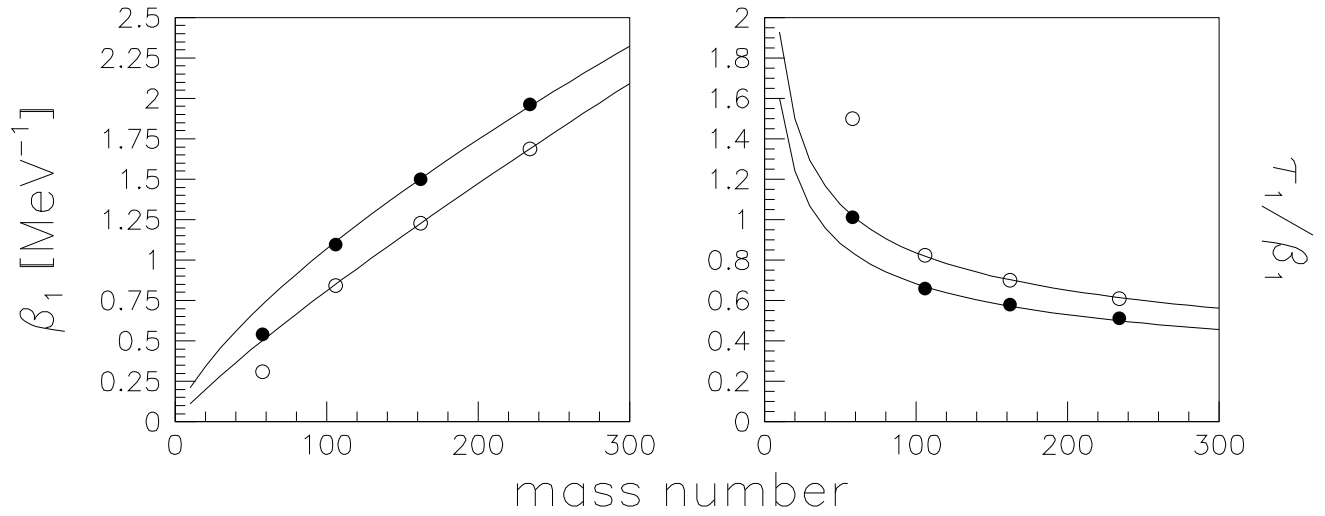


FIG. 9. Evolution of the parameters  $\beta_1$  and  $\tau_1/\beta_1$  of the pairing phase transition with respect to the mass number  $A$ , i.e., the relevant size of the system under study. The full symbols are for the even systems, the open symbols stand for the odd systems. The points for  $^{58,59}\text{Fe}$  are not taken into account in the fit, since for the iron data, a single-particle level spacing  $\epsilon$  off the global systematics is used.